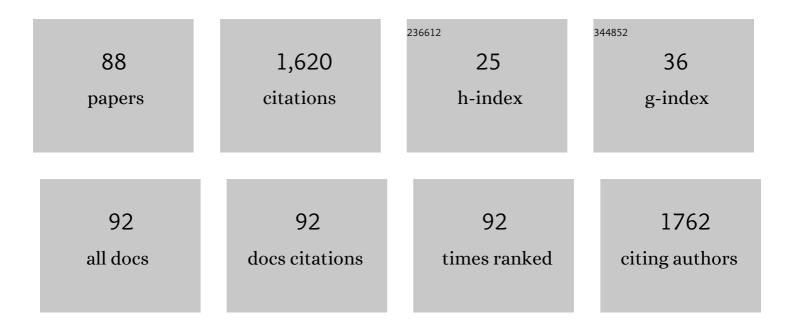
## Lucia Romano

List of Publications by Year in descending order

Source: https://exaly.com/author-pdf/6078891/publications.pdf Version: 2024-02-01



#	Article	IF	CITATIONS
1	Photocatalytical and antibacterial activity of TiO2 nanoparticles obtained by laser ablation in water. Applied Catalysis B: Environmental, 2015, 165, 487-494.	10.8	109
2	Immobilization of nanomaterials in PMMA composites for photocatalytic removal of dyes, phenols and bacteria from water. Journal of Photochemistry and Photobiology A: Chemistry, 2016, 321, 1-11.	2.0	71
3	Nanostructuring in Ge by self-ion implantation. Journal of Applied Physics, 2010, 107, .	1.1	66
4	An enhanced photocatalytic response of nanometric TiO <sub>2</sub> wrapping of Au nanoparticles for eco-friendly water applications. Nanoscale, 2014, 6, 11189-11195.	2.8	58
5	TiO2-coated nanostructures for dye photo-degradation in water. Nanoscale Research Letters, 2014, 9, 458.	3.1	55
6	Novel approach to the fabrication of Au/silica core–shell nanostructures based on nanosecond laser irradiation of thin Au films on Si. Nanotechnology, 2012, 23, 045601.	1.3	52
7	Metal assisted chemical etching of silicon in the gas phase: a nanofabrication platform for X-ray optics. Nanoscale Horizons, 2020, 5, 869-879.	4.1	50
8	Heavy residue excitation functions for the collisions6,7Li+64Zn near the Coulomb barrier. Physical Review C, 2013, 87, .	1.1	45
9	Towards sub-micrometer high aspect ratio X-ray gratings by atomic layer deposition of iridium. Microelectronic Engineering, 2018, 192, 19-24.	1.1	39
10	Nanoscale manipulation of Ge nanowires by ion irradiation. Journal of Applied Physics, 2009, 106, .	1.1	38
11	High-level incorporation of antimony in germanium by laser annealing. Journal of Applied Physics, 2010, 108, .	1.1	38
12	Towards a laser fluence dependent nanostructuring of thin Au films on Si by nanosecond laser irradiation. Applied Surface Science, 2012, 258, 9128-9137.	3.1	37
13	Self-assembly nanostructured gold for high aspect ratio silicon microstructures by metal assisted chemical etching. RSC Advances, 2016, 6, 16025-16029.	1.7	37
14	Towards the Fabrication of High-Aspect-Ratio Silicon Gratings by Deep Reactive Ion Etching. Micromachines, 2020, 11, 864.	1.4	36
15	Microfabrication of X-ray Optics by Metal Assisted Chemical Etching: A Review. Micromachines, 2020, 11, 589.	1.4	36
16	Nanoporosity induced by ion implantation in deposited amorphous Ge thin films. Journal of Applied Physics, 2012, 111, .	1.1	35
17	Fe ion-implanted TiO2 thin film for efficient visible-light photocatalysis. Journal of Applied Physics, 2014, 116, .	1.1	35
18	C ion-implanted TiO2 thin film for photocatalytic applications. Journal of Applied Physics, 2015, 117, .	1.1	35

2

**LUCIA ROMANO** 

#	Article	IF	CITATIONS
19	Effect of isopropanol on gold assisted chemical etching of silicon microstructures. Microelectronic Engineering, 2017, 177, 59-65.	1.1	35
20	High sensitivity X-ray phase contrast imaging by laboratory grating-based interferometry at high Talbot order geometry. Optics Express, 2021, 29, 2049.	1.7	35
21	Nanoscale amorphization, bending and recrystallization in silicon nanowires. Applied Physics A: Materials Science and Processing, 2011, 102, 13-19.	1.1	33
22	Highâ€Aspectâ€Ratio Grating Microfabrication by Platinumâ€Assisted Chemical Etching and Gold Electroplating. Advanced Engineering Materials, 2020, 22, 2000258.	1.6	32
23	Fluorine segregation and incorporation during solid-phase epitaxy of Si. Applied Physics Letters, 2005, 86, 121905.	1.5	30
24	A generalized quantitative interpretation of dark-field contrast for highly concentrated microsphere suspensions. Scientific Reports, 2016, 6, 35259.	1.6	27
25	PMMA/TiO2 nanotubes composites for photocatalytic removal of organic compounds and bacteria from water. Materials Science in Semiconductor Processing, 2016, 42, 58-61.	1.9	27
26	High aspect ratio metal microcasting by hot embossing for X-ray optics fabrication. Microelectronic Engineering, 2017, 176, 6-10.	1.1	27
27	High-temperature annealing of thin Au films on Si: Growth of SiO2 nanowires or Au dendritic nanostructures?. Applied Physics Letters, 2012, 100, .	1.5	26
28	Optical Properties of Nanoporous Germanium Thin Films. ACS Applied Materials & Interfaces, 2015, 7, 16992-16998.	4.0	24
29	Nanoporosity Induced by Ion Implantation in Germanium Thin Films Grown by Molecular Beam Epitaxy. Applied Physics Express, 2012, 5, 035201.	1.1	22
30	UV-black rutile TiO2: An antireflective photocatalytic nanostructure. Journal of Applied Physics, 2015, 117, 074903.	1.1	22
31	Carrier concentration and mobility in B doped Si1â^'xGex. Materials Science and Engineering B: Solid-State Materials for Advanced Technology, 2003, 102, 49-52.	1.7	20
32	Pushing the Limits of Bottom-Up Gold Filling for X-ray Grating Interferometry. Journal of the Electrochemical Society, 2020, 167, 132504.	1.3	20
33	High-aspect ratio silicon structures by displacement Talbot lithography and Bosch etching. Proceedings of SPIE, 2017, , .	0.8	18
34	Room-temperature boron displacement in crystalline silicon induced by proton irradiation. Applied Physics Letters, 2005, 86, 081906.	1.5	17
35	Sub-barrier radioactive ion beam investigations using a new methodology and analysis for the stacked target technique. Physical Review C, 2015, 92, .	1.1	17
36	Quantitative determination of depth carrier profiles in ion-implanted Gallium Nitride. Nuclear Instruments & Methods in Physics Research B, 2007, 257, 336-339.	0.6	16

**LUCIA ROMANO** 

#	Article	IF	CITATIONS
37	TiO2 nanowires on Ti thin film for water purification. Materials Science in Semiconductor Processing, 2016, 42, 24-27.	1.9	15
38	Hot embossing of Au- and Pb-based alloys for x-ray grating fabrication. Journal of Vacuum Science and Technology B:Nanotechnology and Microelectronics, 2017, 35, .	0.6	14
39	Fabrication of X-ray Gratings for Interferometric Imaging by Conformal Seedless Gold Electroplating. Micromachines, 2021, 12, 517.	1.4	14
40	Effect of Strain on the Carrier Mobility in Heavily Dopedp-Type Si. Physical Review Letters, 2006, 97, 136605.	2.9	13
41	Substitutional B in Si: Accurate lattice parameter determination. Journal of Applied Physics, 2007, 101, 093523.	1.1	13
42	Nanoporous Ge electrode as a template for nano-sized ( < 5 nm) Au aggregates. Nanotechnology, 2012, 23, 395604.	1.3	13
43	Optimization of displacement Talbot lithography for fabrication of uniform high aspect ratio gratings. Japanese Journal of Applied Physics, 2021, 60, SCCA01.	0.8	12
44	Optoelectronic properties of nanoporous Ge layers investigated by surface photovoltage spectroscopy. Microporous and Mesoporous Materials, 2014, 196, 175-178.	2.2	11
45	Influence of microstructure on voids nucleation in nanoporous Ge. Materials Letters, 2013, 96, 74-77.	1.3	10
46	Lattice location and thermal evolution of small B complexes in crystalline Si. Applied Physics Letters, 2005, 87, 201905.	1.5	9
47	Mechanism of de-activation and clustering of B in Si at extremely high concentration. Nuclear Instruments & Methods in Physics Research B, 2006, 253, 50-54.	0.6	9
48	Role of the strain in the epitaxial regrowth rate of heavily doped amorphous Si films. Applied Physics Letters, 2008, 93, .	1.5	9
49	Laboratory X-ray interferometry imaging with a fan-shaped source grating. Optics Letters, 2021, 46, 3693.	1.7	9
50	High aspect ratio tilted gratings through local electric field modulation in plasma etching. Applied Surface Science, 2022, 588, 152938.	3.1	9
51	Electrical Activation and Carrier Compensation in Si and Mg Implanted GaN by Scanning Capacitance Microscopy. Solid State Phenomena, 2008, 131-133, 491-496.	0.3	8
52	Amorphization of Si using cluster ions. Journal of Vacuum Science & Technology B, 2009, 27, 597.	1.3	8
53	p-type conduction in ion-implanted amorphized Ge. Materials Science in Semiconductor Processing, 2012, 15, 703-706.	1.9	8
54	Photoactive layered nanocomposites obtained by direct transferring of anodic TiO 2 nanotubes to commodity thermoplastics. Applied Surface Science, 2017, 399, 451-462.	3.1	8

Lucia Romano

#	Article	IF	CITATIONS
55	Development of X-band accelerating structures for high gradients. Chinese Physics C, 2012, 36, 639-647.	1.5	7
56	A Combined Ion Implantation/Nanosecond Laser Irradiation Approach towards Si Nanostructures Doping. Journal of Nanotechnology, 2012, 2012, 1-6.	1.5	7
57	Molybdenum sputtering film characterization for high gradient accelerating structures. Chinese Physics C, 2013, 37, 097005.	1.5	7
58	Influence of point defects injection on the stability of a supersaturatedGaâ€Sisolid solution. Physical Review B, 2005, 71, .	1.1	6
59	Carrier mobility and strain effect in heavily doped p-type Si. Materials Science and Engineering B: Solid-State Materials for Advanced Technology, 2006, 135, 220-223.	1.7	6
60	Nanoporous Ge coated by Au nanoparticles for electrochemical application. Electrochemistry Communications, 2013, 30, 83-86.	2.3	6
61	Development of Laboratory Grating-based X-ray Phase Contrast Microtomography for Improved Pathology. Microscopy and Microanalysis, 2018, 24, 192-193.	0.2	6
62	Boron lattice location in room temperature ion implanted Si crystal. Materials Science and Engineering B: Solid-State Materials for Advanced Technology, 2005, 124-125, 249-252.	1.7	5
63	Room-temperature B off-lattice displacement and electrical deactivation induced by H and He implantation. Nuclear Instruments & Methods in Physics Research B, 2006, 249, 181-184.	0.6	5
64	Single-crystal TiO <sub>2</sub> nanowires by seed assisted thermal oxidation of Ti foil: synthesis and photocatalytic properties. RSC Advances, 2016, 6, 55490-55498.	1.7	5
65	High-intensity x-ray microbeam for macromolecular crystallography using silicon kinoform diffractive lenses. Applied Optics, 2018, 57, 9032.	0.9	5
66	Fabrication of a fractal pattern device for focus characterizations of X-ray imaging systems by Si deep reactive ion etching and bottom-up Au electroplating. Applied Optics, 2022, 61, 3850.	0.9	5
67	Electrical activation and lattice location of B and Ga impurities implanted in Si. Nuclear Instruments & Methods in Physics Research B, 2004, 219-220, 727-731.	0.6	4
68	Physical insight into the phenomenon of B clustering in Si at room temperature. Nuclear Instruments & Methods in Physics Research B, 2007, 257, 146-151.	0.6	4
69	Structural and optical properties of solid-state synthesized Au dendritic structures. Applied Surface Science, 2014, 296, 177-184.	3.1	4
70	Formation and evolution of small B clusters in Si: Ion channeling study. Physical Review B, 2010, 81, .	1.1	3
71	Activation and thermal stability of ultra-shallow B+-implants in Ge. Journal of Applied Physics, 2012, 112, 123525.	1.1	3
72	Impurities–Si interstitials interaction in Si doped with B or Ga during ion irradiation. Journal of Physics Condensed Matter, 2005, 17, S2279-S2284.	0.7	2

**LUCIA ROMANO** 

#	Article	IF	CITATIONS
73	Cross section of the interaction between substitutional B and Si self-interstitials generated by ion beams. Journal of Physics Condensed Matter, 2005, 17, S2273-S2277.	0.7	2
74	Fluorine incorporation during Si solid phase epitaxy. Nuclear Instruments & Methods in Physics Research B, 2006, 242, 614-616.	0.6	2
75	Group III impurities – Si interstitials interaction caused by ion irradiation. Nuclear Instruments & Methods in Physics Research B, 2006, 242, 646-649.	0.6	2
76	Lattice strain of B–B pairs formed by He irradiation in crystalline Si1â"xBx/Si. Nuclear Instruments & Methods in Physics Research B, 2006, 253, 55-58.	0.6	2
77	<i>In situ</i> thermal evolution of B–B pairs in crystalline Si: a spectroscopic high resolution x-ray diffraction study. Journal of Physics Condensed Matter, 2008, 20, 175215.	0.7	2
78	Structural and morphological characterization of Mo coatings for high gradient accelerating structures. Journal of Physics: Conference Series, 2013, 430, 012091.	0.3	2
79	Role of Si self-interstitials on the electrical de-activation of B doped Si. Nuclear Instruments & Methods in Physics Research B, 2006, 242, 656-658.	0.6	1
80	Amorphous–crystalline interface evolution during Solid Phase Epitaxy Regrowth of SiGe films amorphized by ion implantation. Nuclear Instruments & Methods in Physics Research B, 2007, 257, 270-274.	0.6	1
81	Correlation Between Structural and Sensing Properties of Carbon Nanotube-Based Devices. Lecture Notes in Electrical Engineering, 2015, , 207-210.	0.3	1
82	Structural characterization and oxygen concentration profiling of a Co/Si multilayer structure. Nuclear Instruments & Methods in Physics Research B, 2004, 219-220, 732-736.	0.6	0
83	B implanted at room temperature in crystalline Si: B defect formation and dissolution. Materials Science and Engineering B: Solid-State Materials for Advanced Technology, 2005, 124-125, 253-256.	1.7	0
84	Characterisation of solid-phase-epitaxy of amorphous germanium thin-films. , 2012, , .		0
85	Millisecond infrared laser irradiation of SiO <inf>x</inf> N <inf>y</inf> : the role of nitrogen in the photoluminescence emission. , 2014, , .		0
86	Measuring fusion excitation functions with RIBs: A thorough analysis of the stacked target technique and the related problems. AIP Conference Proceedings, 2015, , .	0.3	0
87	Measuring fusion excitation functions with RIBs using the stacked target technique: Problems and possible solutions. EPJ Web of Conferences, 2016, 117, 06013.	0.1	0
88	Editorial for the Special Issue on Micro- and Nano-Fabrication by Metal Assisted Chemical Etching. Micromachines, 2020, 11, 988.	1.4	0